ELSEVIER

Dyes and Pigments 46 (2000) 129–137

DYES and PIGMENTS

Dimerization of Cibacron Blue F3GA and other dyes: influence of salts and temperature

Gaetano Alberghina [a,*], Roberto Bianchini [b], Maria Fichera [a], Salvatore Fisichella [a]

[a] *Dipartimento di Scienze Chimiche, Università di Catania, Viale A. Doria 6, Catania 95125, Italy*
[b] *Dipartimento di Chimica Organica U. Schiff, Università di Firenze, Via G. Capponi 9, Firenze 50121, Italy*

Received 26 February 1999; received in revised form 9 October 1999; accepted 24 January 2000

Abstract

The monomer–dimer equilibria of Cibacron Blue F3GA (CB) and five other dyes (Levafix Brilliant Blue EB, Reactive Scarlet 017, Methyl Orange, Basic Blue 3 and Chicago Blue Sky) have been investigated in water and in the presence of KH_2PO_4. Aggregation of CB has been also examined in the presence of NaH_2PO_4, LiCl and KCl. When a new iterative approach, based on non-linear least-square (NLLSQ) fitting procedure was applied, it was found that the dimerization constants depend on the extension of organic molecules and the number of sulphonic groups. In the case of CB, cations had a greater effect on the equilibrium than anions. Analysis of the calculated spectra for monomer and dimer of Basic Blue 3 after deconvolution allowed us to specify the geometry of the dimer.

Keywords: Dyes; Aggregation; Cibacron Blue F3GA; Deconvolution; Spectrophotometry; Computation

1. Introduction

More than 100 commercial textile dyes have been used in the past few years as synthetic affinity ligands, including agents for separating and purifying proteins through affinity chromatography. The suitable synthetic dyes are able to separate diverse classes of proteins, stable over a wide pH range, exhibit minimal leakage, and can be autoclaved [1,2].

Cibacron Blue F3GA (**1**) is the most often used dye in the preparation of insoluble matrices for affinity chromatography of enzymes and proteins and monitoring the alteration of proteins structures in solution [3–5]. While the protein–dye binding equilibrium is frequently investigated using spectrophotometric techniques to obtain quantitative results, the aggregation of dye molecules can influence the results [6]. A study of the interaction of dye **1** with glutamine syntetase in aqueous solution [7] showed that certain features in the difference spectra that were obtained at different dye concentrations might be due to a shift in the equilibrium between monomers and dimers. In addition, the aggregation of dye **1** has been studied using MO calculations, but the calculated spectra of the monomer and dimer exhibited absorption bands that differed by 100–120 nm relative to the experimental spectra [8].

* Corresponding author. Fax: +39-95-580138.
E-mail addresses: galberghina@dipchi.unict.it (G. Alberghina), bianchini@cesit1.unifi.it (R. Bianchini)

0143-7208/00/$ - see front matter
PII: S0143-7208(00)00045-0

We recently determined the formation constants for the Methyl Orange–human serum albumin complexation and for the Levafix dye with human and bovine serum albumine [9,10]. High dye–protein concentration ratios were used in these studies, so that dye stacking could have two significant effects on the results obtained from spectral data. The first arises from differences between the absorption spectra of stacked and unstacked dye. The second originates from the effects of stacking on the concentration of dye available for binding. To avoid these problems we employed circular dichroism because it is not sensitive to dye aggregation.

In this paper, we report the dimerization of Cibacron Blue F3GA (**1**), Levafix Blue EB (**2**) and Reactive Scarlet 017 (**3**) Methyl Orange (**4**), Basic Bue 3 (**5**), and Chicago Blue Sky (**6**). Dye **1** and other dyes of the Levafix series are often used in affinity chromatography and have been used as model compounds in equilibrium interactions with albumine in aqueous solutions [1,10].

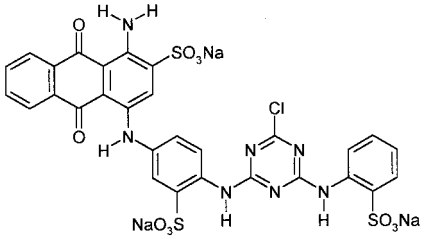

Cibacron Blue F3GA **1**

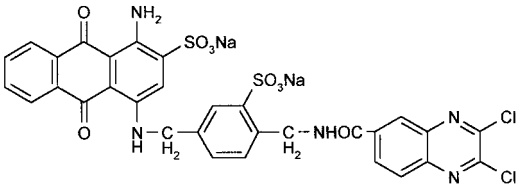

Levafix Brilliant Blue EB **2**

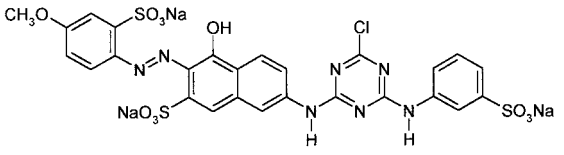

Reactive Scarlet 017 **3**

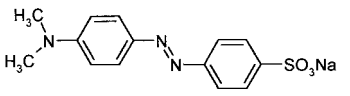

Methyl Orange **4**

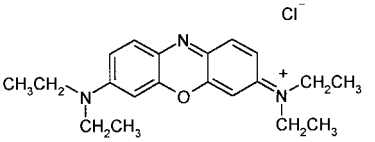

Basic Blue 3 **5**

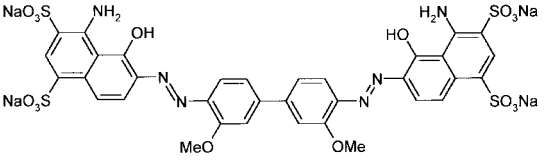

Chicago Blue Sky **6**

2. Experimental section

2.1. Materials

CB (Fluka), Levafix Brilliant Blue EB (Bayer), Reactive Scarlet 017 (ReAcna) were purified on Sephadex LH-20 using MeOH/H_2O (60/40 v/v) [11]. The other dyes were purchased from Aldrich Chemicals and recrystallised several times from MeOH/H_2O (60/40). Dye purity was confirmed by elemental analysis and thin layer chromatography. NaH_2PO_4 and $NaKH_2PO_4$ were purchased from C. Erba (Italy).

2.2. Spectrophotometric measurements

Solutions of the dye were prepared in water, with or without salt, at 10–12 different concentrations (1×10^{-6}–1×10^{-2} M). UV/visible spectra were recorded on a Perkin Elmer Lambda 2S or on a thermostatted Cary 220 UV/visible spectrophotometer, using 10-, 1-, 0.1- or 0.01-cm quartz cells.

2.3. Data fitting procedures

Sets of UV/visible absorption spectra were measured in water at 25°C at various concentrations. Almost 100 experimental points were recorded for each solution, with the absorbance measured at 5 nm intervals over the 230–720 nm range. The spectral changes were described by the dimerization equilibrium shown in Eq. (1),

$$2M \rightleftharpoons D \tag{1}$$

and the association constant can be written as shown in Eq. (2)

$$K_a = [D]/[M]^2 \tag{2}$$

where $[M]$ and $[D]$ are the equilibrium concentrations for the monomer and dimer, respectively, when $[\text{dye}]_{\text{total}} = [M] + 2[D]$. The molar absorptivities (ε) of the solutions are the sum of the contribution of monomer and dimer species:

$$\varepsilon_{\text{exp}} = \varepsilon_1 X_1 + \varepsilon_2/2(1 - X_1) \tag{3}$$

X_1 being the molar fraction of the monomer.

The fitting of the overall set of data was optimised by non-linear least square minimization of the sum of the squared residuals of absorbances to a model that accounts for dimer formation and that is based on Eq. (1). Thus, the dimerization constant (K_a) and the absorbance spectrum of the (at $\lambda_1 \ldots \lambda_m$) are the fitting parameters. The standard deviations of the above parameters and their correlation coefficients are included in the fitting outputs. Even though the problem to be solved seems straightforward, since only a single complex needs to be taken into account, difficulties arise from the small differences between the spectra of M and D. Specific details concerning the experimental approach have been published [12].

The data set for dye **1** in water consists of nearly 2500 experimental data points (absorbance values) collected at 5 nm intervals from 230 to 720 nm, at 9 concentrations and 4 temperatures (10, 25, 50 and 70°C). In NaH_2PO_4 solution 3500 data points were collected. The fitting parameters were the association constants and the molar absorptivities for the monomer and dimer species. Similar data sets were employed in the fitting procedure for dye **2,** while more limited data sets were used in the case of dye **1** in LiCl, NaH_2PO_4 and KCl solutions, and to treat the dimerization of dyes **3–6**.

2.4. Deconvolution

To define the structure of dye **5** using exciton theory [13,14], the calculated electronic spectra for its monomeric and dimeric forms were resolved into the constituent bands, assuming Gaussian curves [15] for the individual bands, and using a least squares fitting program [16].

3. Results and discussion

3.1. The method

In previous approaches, the molar absorptivities of dye monomers and dimers had to be estimated prior to determining aggregation constants. This was achieved by direct extrapolation at the lowest and highest attainable dye concentrations, respectively [17,18]. According to the Hamada approach, only the absorption spectrum of the monomer is required for the calculation method [19,20]. While iterative computer programs have been used to determine monomer and dimer absorptivities in the aggregation of arylazonaphthols [21], the absorption spectrum of the dimer was obtained by fitting spectrophotometric data at the wavelength in which the change in extinction coefficient was the largest upon increasing dye concentration. More reliable results were obtained with a fitting program that uses data collected at all wavelengths. In this case, K_a was varied as an arbitrary parameter until the value that gave the smallest root-mean-square deviations of the optical density data was obtained [22–24].

The computational approach used in the present study has been applied successfully in the determination of thermodynamic and spectral complexation parameters from overlapping bands

involving multiple interactions between Methyl Orange and Levafix Blue EB and human serum albumine [9,10]. It uses all absorption data collected at various wavelengths and does not require monomer or dimer absorptivities. The reproducibility of the experimental curves can be observed in Fig. 1.

The calculated association constants, ΔH_a° and ΔS_a° are reported in Table 1, and Figs. 2–7 provide examples of calculated spectra of monomers and dimers of dyes **1–6**.

The present results were obtained from an experiment involving dyes **1** and **2**, in which a large set of data was recorded at different temperatures, concentrations, optical path lenghts, and wavelengths, using the least squares program. The mean standard deviations of the fits were in the range of 0.022–0.035 absorbance units, and the calculated data were practically coincident with experimental values (Fig. 1a and b), in spite of small differences between the spectra of the monomer and dimer [25].

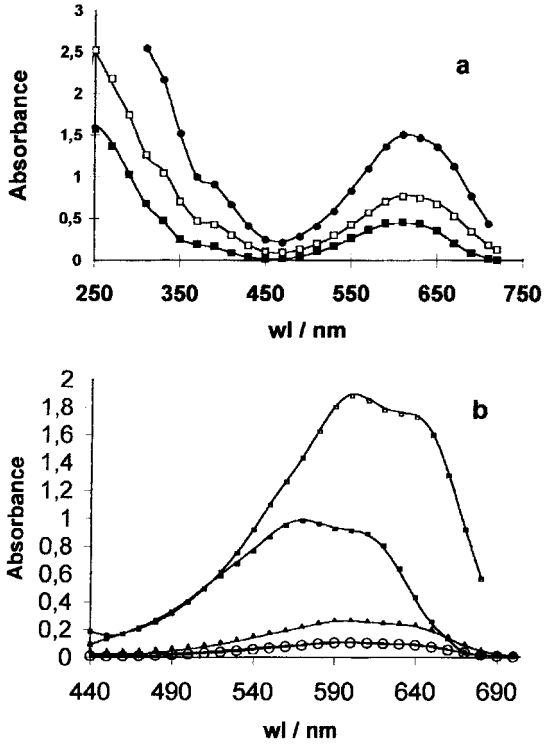

Fig. 1. (a) UV/ visible absorption spectra of dye (**1**) in water. Computed (solid line) and experimental spectra for 50 μM, $d=1$ cm (■), 200 μM, $d=0.5$ cm (□), 2 mM, $d=0.01$ cm (●). (b) UV/visible absorption spectra of dye (**2**) in water. Computed (solid line) and experimental spectra for 300 μM, $d=1$ cm (□), 158 μM, $d=1$ cm (■), 15 M, $d=2$cm (▲), 15.8 M, $d=2$ cm (○).

3.2. Aggregation phenomena: Cibacron Blue F3GA (1)

Spectrophotometric data and the van't Hoff equation were used to calculate the enthalpy change (ΔH_f°). The standard Gibbs energy and entropy changes were calculated using the well known Eqs (4) and (5), the results of which are provided in Table 1.

$$\Delta G^\circ = -\ RT\ \ln\ K_a \tag{4}$$

$$\Delta S_a = (\Delta H_a^\circ - \Delta G^\circ)/T \tag{5}$$

The calculated enthalpy and entropy values are in agreement with the values normally observed for hydrogen bond formation, and are consistent

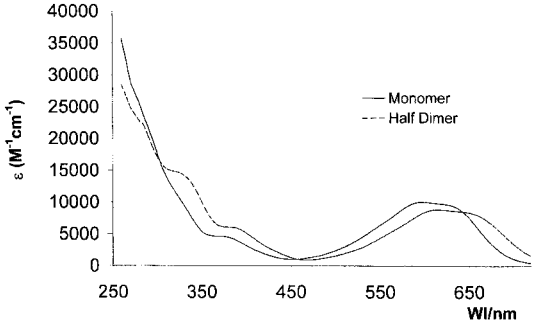

Fig. 2. Monomer and dimer spectra of the dye (**1**) in water.

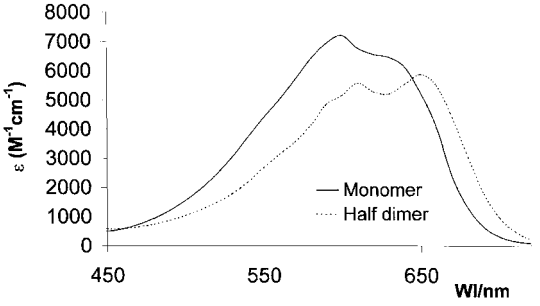

Fig. 3. Monomer and dimer spectra of the dye (**2**) in water.

Table 1
Aggregation constant of several dyes obtained through fitting approach to large visible spectrophotmetric data sets; the standard deviations are reported in parentheses

Dye	K_f at 25°C (M^{-1})	ΔH_a° (kcal mol^{-1})	ΔS_a° (e.u.)	Ambient
1	2900 (500)	−10.9 (4.1)	−20.9 (5.1)	Water
	79 000 (11000)	−13.4 (5.1)	−22.4 (6.3)	NaH_2PO_4
	37 000 (8000)			KH_2PO_4
	14 000 (2000)			KCl
	60 000 (8000)			LiCl
2	485 (1)	−5.87 (0.3)	−7.4 (0.6)	Water
	6211 (4)	−14.2 (0.4)	−30.4 (1.5)	KH_2PO_4
3	1964 (196)			Water
	47 498 (3830)			KH_2PO_4
4	97 (18)			Water
	371 (85)			KH_2PO_4
5	369 (38)			Water
	502 (103)			KH_2PO_4
6	2627 (77)			Water
	4637 (125)			KH_2PO_4

with the values found for the association of similar stuctures [26]. The enthalpy determination took into consieration the sum of phenomena such as the loss of hydrogen bonding, heat of dissociation of dimers, and interaction energy. It also included the heat of solution for monomers and dimers.

Various mechanisms [27] have been suggested to explain the forces of attraction between dye ions in solution. These aggregation phenomena have been attributed to van der Waals forces, ion–dipole and dipole–dipole interactions, and dispersion forces arising from delocalised π electrons. The mutual repulsion forces are reduced by the inclusion of the positively charged gegen ions, and this effect is more favourable when salt is added [25]. The degree to which these forces exist determines the equilibrium position for aggregate formation, which also depends on the temperature [28,29]. Results of prior studies, however, suggest that the dye–dye interactions are not the major driving force behind aggregation; instead, strong water–water interactions tend to force the dyes from solution, causing them to aggregate [30]. Recently, this explanation has been questioned [31,32], due to evidence which strongly indicates that water simply accommodates the apolar solute in its original hydrogen-bonded network. Upon increasing the molecular size or the concentration of apolar solute molecules, the number of water molecule is not sufficient to form a complete shell of hydration, leading to the destruction of the

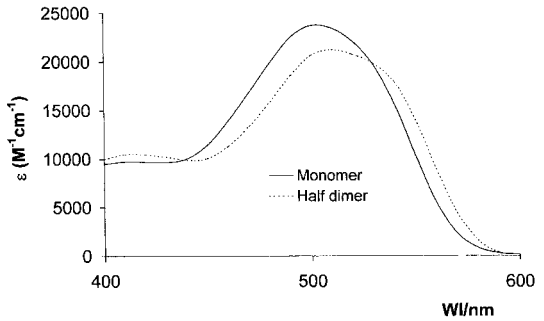

Fig. 4. Monomer and dimer spectra of the dye (**3**) in water.

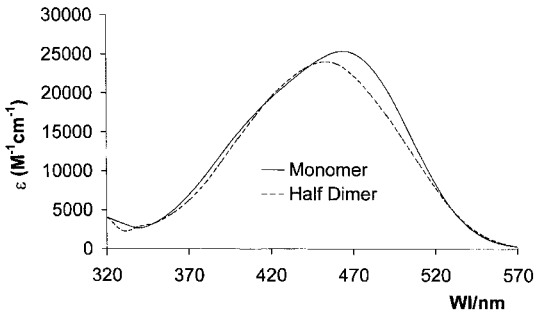

Fig. 5. Monomer and dimer spectra of the dye (**4**) in water.

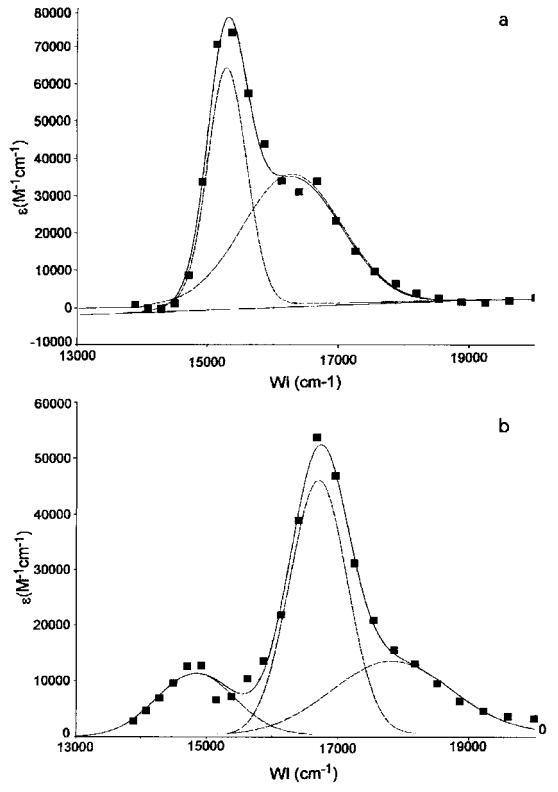

Fig. 6. Deconvolved monomer (a) and dimer (b) spectra of the dye (**5**) in water.

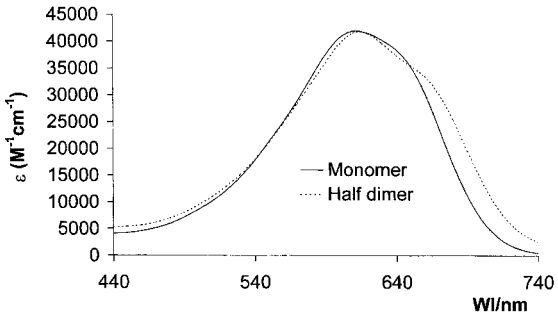

Fig. 7. Monomer and dimer spectra of the dye (**6**) in water.

hydrogen-bonded network. In dilute solutions, the entropy increase associated with aggregation is insufficient to overcome the unfavourable enthalpic effect. In more concentrated solutions, destruction of the shell of hydratation increases the frequency of dye–dye contact, and the tendency to form aggregates of two or more molecules increases significantly [31].

The presence of isosbestic points in the spectra of dye **1** (see Fig. 8, 25°C) indicates that only one equilibrium is operating under the experimental conditions employed. Satisfactory fitting results, in terms of variance and standard deviations, could not be obtained when higher aggregates such as trimers and tetramers were considered, as only complete divergence was observed. The calculated spectra for dyes **1** and **2** (Figs. 2 and 3) indicate that the aggregation process is characterized by a bathocromic shift in the absorption maximum in the 550–650 nm region.

Exciton theory predicts the formation of two bands for the dimer in the excited-state, due to two possible arrangements (in-phase and out-of-phase oscillation) of the transition dipoles of the dimerized chromophore. The relative intensities are a function of the angle between the transition dipoles of the two monomers [20, 21]. Both bands were observed when the molecular units were in parallel planes (parallel plane dimer structure) or in the same plane (oblique plane dimer structure) rotated with an angle q between the planar axes. When a red shift was observed on dimerization, a linear head-to-tail or head-to-head arrangement of monomers was observed, with an angle of $\theta = 0°$ and $\theta = 180°$, respectively, in the same plane [33]. An association between one or more sulphonate groups and the electron-deficient amino group of dye molecules can occur, causing limited stacking contributions from the antraquinone moieties. This conclusion is likely, in view of the dye **1** conformation obtained from semiempirical MO calculations [8]. Calculations showed that the dye molecule is far from planarity, occupying at least three different planes, so that an efficient stacking process can be ruled out.

In dimer formation, the mutual repulsive forces are reduced by the inclusion of positively charged gegen ions as well as by the addition of salts. As shown in Table 1, dimerization constants in the presence of 0.1 M salt solutions are larger than those measured in their absence. The influence of cation and anions on aggregations can be accounted for by the effect of salt on hydrophobic interactions, as proposed by Voet, who reported

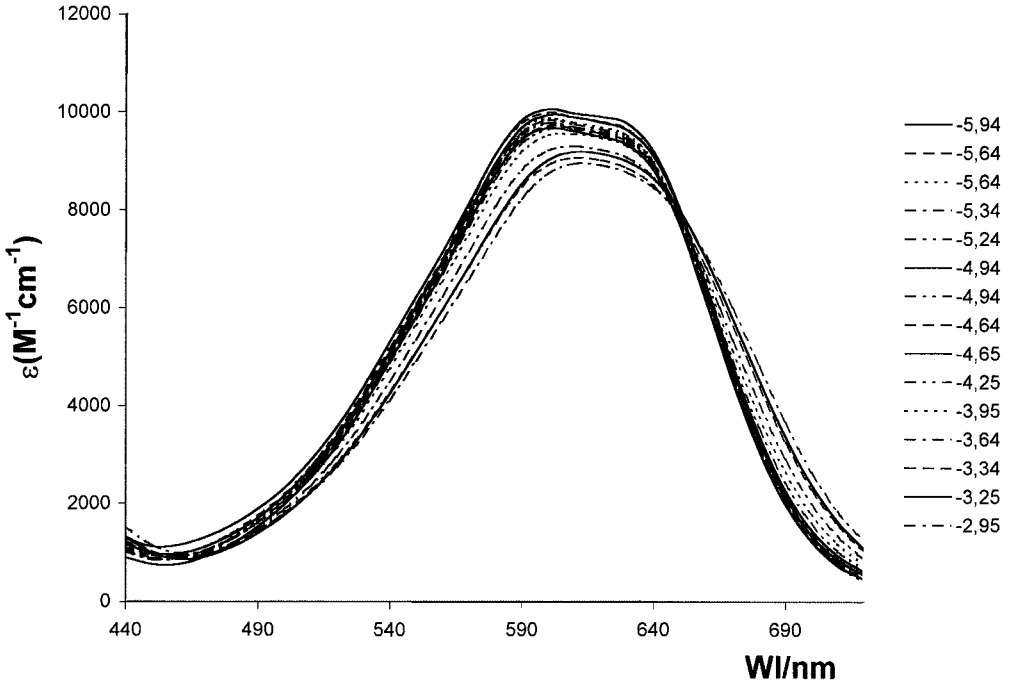

Fig. 8. Visible absorption spectra of dye (**1**) at 25°C in water; in the insert is reported the log of concentrations.

lyotropic numbers for different ions (T values for cations and N values for anions) [34]. Relatively large T values and small N values correspond to a large hydrophobic effect and favour dye aggregation [35]. It is apparent that Li^+ ($T=115$) is more effective on dye aggregation than K^+ ($T=75$) and $H_2PO_4^-$ ($N=8.2$) is more effective than Cl^- ($N=10$). The value found for the KH_2PO_4 dimerization constant is in agreement with this finding.

3.3. Aggregation of dyes **2–6**

The spectrum of the dye **4** dimer shows a 5–10 nm hypsochromic effect, while that for the dye **6** dimer shows a 5 nm bathochromic effect. For all of these dyes the spectra of dimers also reflect a hypocromic effect compared to the monomer. Hypochromic and hypsochromic shifts were observed with the Basic Blue 3 dimer.

Dyes **1**, **3** and **6** are large organic molecules that exhibited a high tendency to dimerise in aqueous media, while smaller dyes **4** and **5** have aggregation constants that are an order of magnitude lower. Dye **2** does not fit into the above categories, because it is as large as dye **1** and has a lower association constant. In this case, it is possible that the methylene groups on each end of the sulphophenyl moiety [36] increase the conformational freedom of the molecule, resulting in a more complex arrangement than in dye **1**, making stacking of the anthraquinone moieties more difficult.

Dyes **1–6** dimerise extensively in buffer solution, with the level of dimerisation depending on the presence of sulphonate groups, which are shielded

Table 2
Excitonic and structural parameters for the dimerisation of dye **5** in water (w) and in phosphate buffer (b)

	ν_M	f_M	ν_H	ν_J	f_H	f_J	α (deg)	R (Å)
w	15 297	0.203	16 723	14 761	0.207	0.019	36	4.9
b	15 297	0.193	16 737	15 039	0.269	0.0691	31	5.1

more effectively in saline solutions. The effect of 0.1 M KH_2PO_4 on aggregation decreased in the order: dyes **1** and **3** (3 sulphonate groups), dye **2** (2 sulphonate groups), dye **4** (1 sulphonate group) and dye **5** (0 sulphonate groups). Dye **6**, which has 4 sulphonate groups, does not fit this pattern, probably because its stacking process involves only the central -*N*=*N*-methoxyphenyl-methoxyphenyl-*N*=*N*- apolar moiety.

3.4. Basic Blue dimer stacking

According to exciton theory, when two dye molecules form a dimer in a parallel plane structure, the absorption peak of the monomer is split into two peaks, namely H and J bands (higher and lower energy, respectively) [20]. This splitting is related to the relative orientations of the two molecules and to the distance between them.

Deconvolution of the calculated absorption spectrum for monomer and dimer in water (Fig. 6) and buffer permitted the calculation of parameters ν_M (monomer peak, cm^{-1}), f_M (monomer oscillator strength), ν_H (dimer H band, cm^{-1}), ν_J (dimer J band, cm^{-1}), and f_H, f_J (H- and J-band oscillator strengths), all of which are reported in Table 2.

According the parallel plane dimer model, justified by the planar geometry of the molecule, the splitting ($\Delta\nu$) between the H and J bands is $\Delta\nu$ (cm^{-1}) = $f(\alpha, R)$, because of dipole–dipole interactions between the two molecules in the dimer [21]. R (Å) is the distance between the two molecules and angle α depends on the orientation of the adjacent molecules.

$$\Delta\nu = \frac{2.14 \times 10^{10} \ (\text{as } \alpha) f}{\nu R^3} \tag{6}$$

The angle is determined from the relative oscillator strengths of the split bands through Eq. (7):

$$\alpha = 2 \ \tan^{-1}(\nu_H f_J / \nu_J f_H)^{1/2} \tag{7}$$

Using Eq. (7) we determined that $\alpha = 36^\circ$ and $R = 4.89$ Å. These values are in good agreement with the data reported in literature for comparable dimers [37–39]. For the dimer in 0.1 M phosphate solution, we found that $\alpha = 31.3^\circ$ and $R = 5.1$ Å. The 5 Å distance and 36° angle are consistent with stacking of the aromatic moieties, which avoids the steric repulsion normally caused by the diethylamino groups.

Acknowledgements

This work was supported by CNR "Progetto Finalizzato Biotecnologie" and MURST "Studio delle Proteine dei cereali e loro relazioni con aspetti tecnologici e nutrizionali".

References

[1] Lowe CR, Burton N, Dilmaghanian S, McLoughlin S, Pearson J, Stewart D. et al. In: Vijalakshmi MA Bertand O, editors. Protein–dye interactions: development and applications. London and New York: Elsevier Applied Science.
[2] Lowe CR, Burton SJ, Clonis YD, Pearson JC. Chromatogr 1986;376:121–30.
[3] Stellwagen E. Acc Chem Res 1977;10:92–8.
[4] Ling TGI, Mattiason B. J Chromatogr 1982;252:159–66.
[5] Johansson G, Joelsson M. J Chromatogr 1991;537:219–33.
[6] Hubble J, Mayes AG, Eisenthal R. Analitica Chimica Acta 1993;279:167–77.
[7] Federici MM, Chock PB, Stadtman ER. Biochemistry 1985;24:647–60.
[8] Edwards RA, Woody RW. J Phys Chem 1983;87:1329–37.
[9] Ambrosetti R, Bianchini R, Fisichella S, Fichera M, Zandomeneghi M. Chem Eur J 1997;2:149–56.
[10] Alberghina R, Bianchini R, Fisichella S, Fichera M, Zandomeneghi M. Gazz Chim Ital 1996;127:577–85.
[11] Burton SJ, McLoughlin SB, Stead CV, Lowe CR. J Chromatogr 1988;435:127–37.
[12] Ambrosetti R, Ricci D, Bianchini R. Gazz Chim Ital 1997;127:567–75.
[13] Monahan AR, Germano NJ, Blossey DF. J Phys Chem 1971;75:1227–33.
[14] Rohatgi KK, Mukhopadhyay AK. J Phys Chem 1972;76:3970–3.
[15] Ott RJ, Widmer U, Zollinger H. J Soc Dyers Colour 1975; 330–5.
[16] Origin 5.0, Microcal™.
[17] Robinowith E, Epstein LF. J Am Chem Soc 1941;63:69–78.
[18] Gosh AK. Physik Chem Neue Folge 1970;94:161–6.
[19] Hamada K, Mitsuishi M. Dyes Pigments 1992;19:161–8.
[20] Hamada K, Fujita M, Mitsuishi M. J Chem Soc Faraday Trans 1990;86:4031–5.
[21] Monahan AR, Blossey DF. J Phys Chem 1970;74:4014–21.

[22] Arbeloa FL, Liebana IR, Fernandez EC, Arbeloa IL. Spectrochimica Acta 1989;45:1201–6.
[23] Sewyn JE, Steinfeld JI. J Phys Chem 1972;76:762–74.
[24] Lamm ME, Neville DM. J Phys Chem 1965;69:3872–7.
[25] Ambrosetti R, Bianchini R, Bellucci G. J Phys Chem 1986;90:6261–6.
[26] Coates E. J Soc Dyers Colour 1969;85:355–68.
[27] Peters RH. Textile chemistry, vol. III, the physical chemistry of dyeing. Amsterdam: Elsevier, 1975. p. 852.
[28] Valdes-Aguileira O, Neckers DC. Acc Chem Res 1989; 22:171–7.
[29] Nemethy G, Sheraga H. J Chem Phys 1962;36:3382–400.
[30] Tanford C. The hydrophobic effect. New York: Wiley Interscience, 1980.
[31] Pratt LR, Chandler D. J Chem Phys 1977;67:3683–704.
[32] Blokzijl W, Engberts JBFN. Angew Chem Int Ed Engl 1993;32:1545–79.
[33] Cantor CR, Schimmel PR. In: W.H. Freeman and Co., editors. Biophysical chemistry, part II. p. 397.
[34] Voet A. Chem Rev 1937;20:169–70.
[35] Yang Y, Ladish CM. Text Res J 1993;63:283–9.
[36] Alberghina G, Babulano GA, Fisichella S, Renda E, Bianchini R, Forte C. Gazz Chim Ital 1997;127:803–8.
[37] Arbeloa IL. J Chem Soc Faraday Trans 2 1981;77:1725–33.
[38] Arbeloa FL, Gonzalez IL, Ojeda PR, Arbeloa IL. J Chem Soc Faraday Trans 2 1982;78:989–94.
[39] Arbeloa IL, Ojeda PR. Chem Phys Letters 1982;87:556–60.